Williamsburg, Virginia
ACTIVE 04
2004 September 20-22

Active Control of Modulated Sounds in a Duct

Vivake Asnani
The Ohio State University
Mechanical Engineering,
Suite 255
650 Ackerman Rd
Columbus, OH 43202
asnani.1@osu.edu

Rajendra Singh
The Ohio State University
Mechanical Engineering,
Suite 255
650 Ackerman Rd
Columbus, OH 43202
singh.3@osu.edu

Stephen Yurkovich
The Ohio State University
Electrical Engineering
408 Dreese Labs
2015 Neil Avenue
Columbus, OH 43210
yurkovich.1@osu.edu

ABSTRACT

Modulated disturbances are often produced by noise sources originating from rotating machinery such as gears, bearings and fans. Such disturbances typically produce frequency side-bands, which along with the main components (such as gear mesh or blade passage frequencies and their harmonics) control the perception of sound. Traditional active noise control schemes tend to attenuate the fundamental signal components, frequently neglecting and sometimes even increasing the amplitudes of side-band structures. In this paper, we describe a new experiment where we study the side-band phenomenon by generating synthesized AM or FM modulated sounds in a duct. An attempt is first made to cancel these sounds using the conventional FX-LMS algorithm. This algorithm converges to a solution where the frequency side-bands seem to become more prevalent. The narrowband adaptive noise equalizer, implemented in the time domain, is examined as a viable alternative. This scheme uses a network of notch filters, each of which operates on a single frequency using an internally generated reference signal. The equalizer method allows independent control of the amplitudes for each operating frequency in the disturbance. Significant success is reported in attenuating the side band structures or shaping them.

1. INTRODUCTION

Modulated noise is often produced by sources with rotating parts such as gears, bearings and fans. These disturbances have a time-varying envelope that may produce a coarse and unpleasant sound. Figure 1a illustrates the time-varying behavior of an amplitude modulated (AM) signal. Often modulated disturbances can be recognized by side-bands in the frequency domain, as shown in Figure 1b. Such disturbances are of significant concern for manufacturers of consumer products (automobiles, power tools, household appliances, etc.) due to their impact on perceived operation and sound quality.[1] Modulated noise is also associated with the non-ideal functioning of rotating machines or components; for this reason side-bands are carefully scrutinized in the machinery diagnostics field for health monitoring purposes.[2]

The problem of active noise control (ANC) has been studied extensively in the last two decades.[3] Multiple schemes have been reported to control the sound fields produced by rotating machinery. Typically the fundamental frequencies are the primary concern and thus the side-band structures that exist in these sound fields are not specifically targeted. For example, Guan et al.[4] developed a system to control the vibration response of a gearbox containing multiple side-bands about the gear mesh frequency. The control scheme successfully reduced the amplitude of the gear mesh frequency by 13 dB, but side-bands around the mesh frequency significantly increased in amplitude. To the best of our knowledge, only one publication, written by Mucci and Singh[5], has specifically addressed the modulated ANC problem. They[5] examined the feasibility of canceling amplitude modulated or frequency modulated (FM) vibration disturbances applied to a structural beam. The basic premise behind studying these disturbances was that the complex spectra produced by geared systems could be synthesized by an appropriate combination of AM and FM functions. Their results included an overall reduction in the fundamental frequencies and side-bands in both the AM and FM spectra. However, the fundamental frequencies were attenuated more aggressively and the residual error contained frequency side-bands comparable to or greater in magnitude than the fundamental components. In this paper, we describe a new experiment where the side-band phenomenon is studied by generating synthesized modulated sounds in a duct. This allows us to easily implement and evaluate alternate control algorithms.

2. PROBLEM FORMULATION

In some applications including those carrying modulated sounds, complete cancellation of the sound field is either not desirable or not possible. For example, the clientele of a sports-car manufacturer would expect to hear the "signature sound" from the high-performance engine, thus complete cancellation of engine noise is not desirable. In the case where complete cancellation is not possible using an active noise controller, the residual noise spectrum may have an undesirable shape. This is often the case when the total mean-squared error is minimized, such as in the Filtered-X LMS (FX-LMS) algorithm. This algorithm was originally proposed by Morgan[6] (1980) and Widrow[7] (1981). It was first used specifically for ANC by Burgess[8] (1981); today the FX-LMS algorithm is widely used in practical ANC applications.[3] The time domain narrowband active noise equalizer (NANE), based on the adaptive notch filter concept[9], was first introduced by Ji and Kuo[10, 11, 12] as a method to control the amplitudes of periodic disturbances containing harmonic components. The algorithm provides a method to control the amplitudes of each harmonic in the residual error spectrum linearly and arbitrarily. A modification to this algorithm was suggested by Diego et al.[13], which enables the NANE to be used to adjust the amplitudes of neighboring frequencies in a disturbance spectrum independently. This modification makes the NANE more useful for controlling quasi-periodic disturbances, such as modulated sound, where the frequency components are not harmonically related and may be closely spaced.

This paper compares the results of implementing the FX-LMS and the NANE algorithms for modulated disturbances. Both algorithms are implemented using an acoustic duct experiment where control may be applied to either resonant or off-resonant regimes. The scope of the experiment is, however, limited to single-input single-output (SISO) control for the sake of simplicity. Similar to Mucci and Singh[5], the disturbances are generated using AM and FM functions. The AM disturbances are of the form:

$$F_{AM}(t) = \sin(\omega_c t)[1+\sin(\omega_m t)] = \mathrm{A}\{\sin(\omega_c t) + \frac{1}{2}\sin[(\omega_c \pm \omega_m)t \pm \frac{\pi}{2}]\},$$

where ω_c is the carrier frequency and ω_m is the modulation frequency. The trigonometric expansion highlights the presence of three frequency components in the spectrum of the AM disturbance; these are the carrier frequency and two side-bands at plus and minus the modulation frequency. Using the same notation, the FM function is written as:

$$F_{FM}(t) = \cos[\omega_c t + \varphi_m \sin(\omega_m t)]$$

$$= J_0(\varphi_m)\cos\omega_c t + \sum_{p=1}^{\infty}(-1)^p J_p(\varphi_m)[\cos(\omega_c - p\omega_m)t + (-1)^p \cos(\omega_c + p\omega_m)t].$$

The expansion shows that this disturbance has an infinite number of side-bands surrounding the carrier frequency component at integer multiples of the modulation frequency. The amplitude of the signal components are controlled by $J_p(\varphi_m)$; this is the Bessel function of the first kind of order p, where the argument is the modulation index, φ_m. For the present study, the modulation index was set at unity.

3. EXPERIMENTAL SYSTEM

A. The Duct Experiment

A duct system was used to perform ANC on single dimensional noise disturbances, facilitating the use of the SISO control schemes. The duct environment with three acoustic cavities is shown in Figure 2. The center cavity is the duct where the disturbance and control sound fields interact. At the rear and top of the main duct are enclosures to house the disturbance speaker and control speaker respectively. These enclosures are identical and serve to improve the low frequency response of the speakers. The duct is closed at both ends to minimize the contaminating effect from the surrounding environment. The width and height of the acoustic duct are small enough so that transverse acoustic modes are not excited below 1225 Hz. The length of the duct was chosen based on the spacing of longitudinal modes in the frequency domain. It is undesirable to have significant modal overlap since modulated disturbances would excite more than one mode, unnecessarily complicating the pressure spectra. Consequently wide spacing between modes is preferred and is accomplished by making the duct relatively short. Unfortunately, a short duct reduces the amount of time available for processing in feed-forward control systems. Also it forces the microphone to be positioned in the near field of the speakers which cannot be controlled effectively with a SISO system. Considering the tradeoff, the duct length was selected to be 0.686 m, which places the first four plane wave modes at 256, 499, 740.5, and 976 Hz.

B. Instrumentation and Hardware

A block diagram of the ANC hardware and instrumentation is shown in Figure 3. The speakers chosen as the disturbance and control sources were Dynaudio MW160's. These are 7" speakers with virtually flat frequency response and very low harmonic distortion in the range from 55 Hz to 3.5 kHz . The speakers are driven by an Elecro-Voice high-fidelity amplifier. A PCB microphone / preamplifier and signal conditioning unit were used to sense the pressure signal at the end of the duct. The dSPACE DS1104 controller board was used to interface with the transducer signals and implement control algorithms in real time. This controller board connects to a PC via the PCI slot on the motherboard. Algorithms can be developed in Simulink and then compiled into assembly language. The assembly code is then sent to flash memory onboard the DS1104 controller board for implementation. The DS1104 utilizes a 250 MHz CPU to run the program in real-time. The controller board interfaces with the analog transducer signals via 16-bit ADCs and DACs.

C. Oversampling Scheme

An oversampling scheme was employed as an alternative to analog anti-aliasing and reconstruction filters. The sampling rate was 20 kHz and the control system operated at 2.5 kHz. Decimation and interpolation were each implemented in two stages using polyphase structures to minimize computational burden. The sampling rate places the first spectral image in the range from 18,775 to 20,000 Hz (corresponding to the range DC – 1225 Hz). This range is greatly attenuated by the action of the zero-order-hold and thus the image does not influence the sound field in the duct.

4. FILTERED-X LMS ALGORITHM APPLIED TO MODULATED DISTURBANCES IN A DUCT

Figure 4 is a block diagram of the FX-LMS algorithm implemented with the oversampling scheme. Our scheme differs from the standard FX-LMS algorithm, in the following manner: The disturbance and control signals (x[n] and y[n] respectively) are interpolated before the DACs and the error signal (e[n]) is decimated after the ADC. Here $\tilde{P}(z)$ and $\tilde{S}(z)$ are the primary and secondary path transfer functions, discretized by their zero-order-hold representation at the high sampling rate. $C(z)$ is the control path transfer function between the output of the adaptive FIR filter, $W(z)$, and e[n]. The standard update equation is used to adjust the coefficients of $W(z)$.

$$\mathbf{w}[n+1] = \mathbf{w}[n] - 2\mu \cdot e[n] \cdot \mathbf{f}_x[n]$$

Here μ is the step size and $f_x[n]$ is the filtered reference signal, which is taken to be the same as the internally generated disturbance signal filtered by the control path estimate. In this system the control path estimate ($\hat{C}(z)$) is a 49 sample delay together with a 21st order IIR filter, and is accurate within two degrees of the control path phase response for most frequencies.

Figure 5 shows the magnitude frequency responses of the primary path ($P(z)$) and control path ($C(z)$) transfer functions, where the first four plane wave modes are distinct. The FIR filter is best suited to model the system zeros, and thus any on-resonance components in the disturbance spectrum are predisposed to control. Accordingly, results are provided for two disturbance cases as outlined in Table 1. In Case 1, the AM and FM disturbances have carrier frequencies corresponding to the first duct system resonance. In Case 2, results are presented where the first side-band (higher in frequency than the carrier) excites the first resonance. The modulation frequency is set at 15 Hz for all results, so the disturbances tend to excite only the first mode.

A. Case 1

Figures 6 shows the result of using the FX-LMS algorithm to attenuate Case 1 AM noise disturbance, for which the carrier frequency excites the first system resonance at 256 Hz. In the uncontrolled state, the carrier frequency is approximately 10 dB higher in amplitude than the two side-bands in the disturbance spectrum. After control is applied, all frequency components are diminished. However the carrier is attenuated more aggressively, resulting in a residual pressure spectrum where it has an amplitude 30 dB less than the side-band structures. The effect of this control on the time-history of the disturbance can be seen in Figure 7. With control, the amplitude of the disturbance is lessened; nevertheless, the beating phenomenon of the modulation envelope is now more distinct.

The results from Case 1 FM disturbance are shown in Figure 8. Ideally there are a countably-infinite set of side-bands in the disturbance spectrum at integer multiples of 15 Hz from the carrier frequency. However, the side-bands with appreciable amplitudes lie mostly in the range from 211 to 301 Hz. The disturbance is attenuated at all frequencies in this range; however the control is most effective at the fundamental (carrier) frequency. Also, it

should be noted that the further the side-bands are away from the fundamental, the less they are attenuated by the controller. The time-history plots in Figure 9 show that the control causes the modulation envelope to become more apparent, unlike the case prior to control.

B. Case 2

The AM disturbance results for Case 2 are presented in Figure 10. The upper side-band is on-resonance and so it is most apt to be modeled by the adaptive FIR filter. Furthermore its amplitude is comparable to the carrier frequency in the disturbance spectrum. However, the fundamental frequency is attenuated most by the controller, while the side-bands are reduced to equal amplitudes. Also, overall attenuation is less than the Case 1 disturbance. The time-history plots in Figure 11 show that the modulation envelope is apparent both before and after control although different characteristics are seen.

The FM results for Case 2 are shown in Figure 12. The fist upper side-band is on-resonance and so its amplitude is comparable to the carrier frequency. The on-resonance side-band received the most attenuation (49 dB) with control and the fundamental frequency was attenuated the second most (37 dB). Also, the upper side-bands have received more attenuation than the respective lower side-bands. This result is not consistent with the trends observed for the other cases. Figure 13 shows the time history of this case, where after control the modulation envelope has both large and small amplitude variations.

5. NANE APPLIED TO MODULATED DISTURBANCES IN A DUCT

A block diagram of the single-frequency NANE, developed by Ji and Kuo[10, 11, 12], is shown in Figure 14. Here the reference signal is an internally generated cosine wave instead of the full-band disturbance signal. The reference signal is split into two branches: (i) an in-phase branch and (ii) a 90 degrees phase-shifted branch. Each branch is weighted by a 1-tap filter that is adjusted using the FX-LMS algorithm. The filter outputs are added together and then split into two output branches; these are the canceling branch and the balancing branch. In the canceling branch the output is gained by the factor $1-\beta$ and then sent through the control path ($C(z)$) to combine with the noise disturbance and create the error signal. In the balancing branch the output is weighted by β, filtered by the control path estimate ($\hat{C}(z)$) and then added to the error signal, such that the FX-LMS algorithm is not affected by the output weighting.

The proposed control system can operate in four modes, depending on the choice of β. When β equals zero, the system is in cancellation mode and an infinite null is created in the closed loop response at the reference frequency. If β is set between zero and one, the system is in attenuation mode and the disturbance will be reduced in amplitude at the reference frequency. When β is set to one, the system is in the neutral mode and doesn't affect the disturbance. If β is set greater than one, the system is in enhancement mode and the disturbance is augmented at the reference frequency.

Diego et al.[13] developed a method to combine multiple single-frequency NANE structures such that the gains at each frequency are independent, as illustrated in Figure 15. Each FX-LMS algorithm in the structure receives the same pseudo-error signal $e'[n]$, where

$$e'[n] = e[n] + \sum_{k=1}^{K} \beta_k \left\{ \hat{c}[n] * y_k[n] \right\}$$

And the filter coefficients of the k[th] branch are updated using

$$w_{ki}[n+1] = w_{ki}[n] - 2\mu e'[n] \left\{ x_{ki}[n] * \hat{c}[n] \right\}, \; i = 1, 2$$

A. Case 1 and 2 Results

Figure 16 through 19 present the results for both Case 1 and 2 disturbances with the NANE in cancellation mode. For all cases the NANE has completely attenuated the disturbances, unlike the FX-LMS algorithms discussed in the previous section. This result shows that the presence of frequency side-bands does not significantly influence the action of the NANE.

B. Spectral Shaping Using NANE

Figure 20 demonstrate the ability of the NANE to independently and arbitrarily control the amplitudes of the components in a noise disturbance. Here $\beta = 0$ for the side-bands and $\beta = 2$ for the fundamental frequency. The

residual error spectrum shows that the fundamental frequency does in fact double in amplitude, while the side-bands are eliminated. This would be practical in the case where audible information was necessary, say for the sake of safety around a rotating machine. Figure 21 shows the effect of this equalizer setting in the time domain. Notice that the control has eliminated variation in the time domain envelope.

6. CONCLUSION AND SUGGESTIONS FOR FUTURE WORK

Modulated disturbances are commonly produced by rotating noise sources such as gears, bearing, and fans. These disturbances are typically identified by frequency side-bands about the primary spectral components. The presence of side-bands often leads to a time-varying envelope (including the beating type) which is generally perceived as objectionable by a human observer. The results of implementing alternate ANC algorithms on modulated sounds have been presented, in the context of an experimental duct system. The FX-LMS algorithm is first implemented as a benchmark case, while the NANE is presented as a viable alternative. The FX-LMS algorithm significantly reduces the total amplitude of both AM and FM disturbances when the carrier frequency is placed on the first acoustic resonance. However the carrier frequencies were attenuated much more than the side-bands and so the beating phenomenon became more apparent. The FX-LMS algorithm applied to the AM disturbance with an on-resonance side-band resulted in much less total attenuation than the on-resonance carrier case. However, the fundamental frequency is still attenuated the most and side-bands are reduced to equal amplitudes. The FX-LMS algorithm applied to an FM disturbance with on-resonance side-band results in very different results. The on-resonance side-band is greatly diminished while the carrier frequency receives the second most attenuation. Furthermore, the upper side-bands receive more attenuation than the respective lower side-bands. Subsequently, the NANE, used in the cancellation mode, is found to completely attenuate all frequency components for all cases of AM and FM disturbances. Additionally, this algorithm was used to linearly shape the error spectrum of an AM disturbance to eliminate the beating phenomenon associated with the side-bands.

Our investigation shows that several interesting future studies are warranted. For example, one might analyze the optimal control studies, implemented in the frequency domain, to understand why the FX-LMS algorithm produces biased residual error spectra for modulated disturbances. Further developments to the NANE concept could include a refined frequency domain based algorithm that would be generally applicable for quasi-periodic disturbances. This algorithm might utilize concepts similar to the frequency domain periodic noise equalizer developed by Kuo et al.[14]. A frequency domain controller would have the advantage of lower computational burden and effective control without prior knowledge of the disturbance frequencies. Finally, such algorithms need to be implemented in practical systems (including geared systems) where more complicated side-band structures are found as simple AM or FM modulation theories may not explain the real-life noise or vibration signals.[2]

7. REFERENCES

1. G. Wesley Blankenship and Rajendra Singh, "New rating indices for gear noise based upon vibro-acoustic measurements," *Noise Control Eng. J.*, **38**(2), 81-92 (1992).

2. G. Wesley Blankenship and Rajendra Singh, "Analytical solution for modulation side-bands associated with a class of mechanical oscillators," *J. of Sound and Vibration*, **179**(1), 13-36 (1995).

3. S. M. Kuo and D. R. Morgan, "Active noise control: A tutorial review," *Proc. of the IEEE* (June 1999), **87**(6) pp. 943-973.

4. H. Guan, T.C. Lim, and W.S. Shepard Jr., "Experimental study of active vibration control of a gearbox system," Submitted to *J. of Sound and Vibration.*, (in-press, submitted 2003).

5. Peter Mucci and Rajendra Singh, "Active vibration control of a beam subjected to AM or FM disturbances," *Noise Control Eng. J.*, **43**(5), 159-171 (1995).

6. D. R. Morgan, "An analysis of multiple correlation cancellation loops with a filter in the auxiliary path," *IEEE Trans. Acoust., Speech, Signal Processing*, ASSP-**28**, 454-467 (1980).

7. B. Widrow, D. Shur, and S. Shaffer, "On adaptive inverse control," *Proc. 15th Asilmar* Conf (1981), pp. 185-189.

8. J. C. Burges, “Active adaptive sound control in a duct: A computer simulation,” *J. Acoust. Soc Amer.*, **70**(3), 715-725, (1981).

9. B. Widro, et al, “Adaptive noise canceling: principles and applications,” *Proc. of IEEE* (Dec 1975), **63**(12), pp. 1692-1716.

10. Min J. Ji, and Sen M. Kuo, “An active harmonic noise equalizer,” *Proc. ICASSP-93*. (1993), **1,** pp. 189-192.

11. Min J. Ji, and Sen M. Kuo, “Principle and application of adaptive noise equalizer,” *IEEE Trans. on Circuits and System-II: Analog and digital Signal Processing*, **41**(7), 471-474 (July 1994).

12. Min J. Ji, and Sen M. Kuo, “Development and analysis of an adaptive noise equalizer,” IEEE *Trans. Acoust., Speech, Signal Processing*, **3**(3), 217-222 (1995).

13. M. de Diego, A. Gonzalez, C. García, M. Ferrer, “Some practical insights in multichannel active noise control equalization,” *Proc. ICASSP-2000* (June 200), pp. 837-840.

14. Sen M. Kuo, Mansour Tahernezhadi, and Li Ji, “Frequency-domain periodic active noise control and equalization,” *IEEE Trans. Acoust., Speech, Signal Processing*, **5**(4), 348-358 (1997).

8. FIGURES AND TABLES

Modulation Type	Carrier and modulation frequencies	
	Case 1	Case 2
AM	$f_c = 256$ Hz $f_m = 15$ Hz	$f_c = 241$ Hz $f_m = 15$ Hz
FM	$f_c = 256$ Hz $f_m = 15$ Hz	$f_c = 241$ Hz $f_m = 15$ Hz

Table 1: List of AM and FM modulations used for noise disturbances. Note that the first natural frequency of the duct system is at 256 Hz.

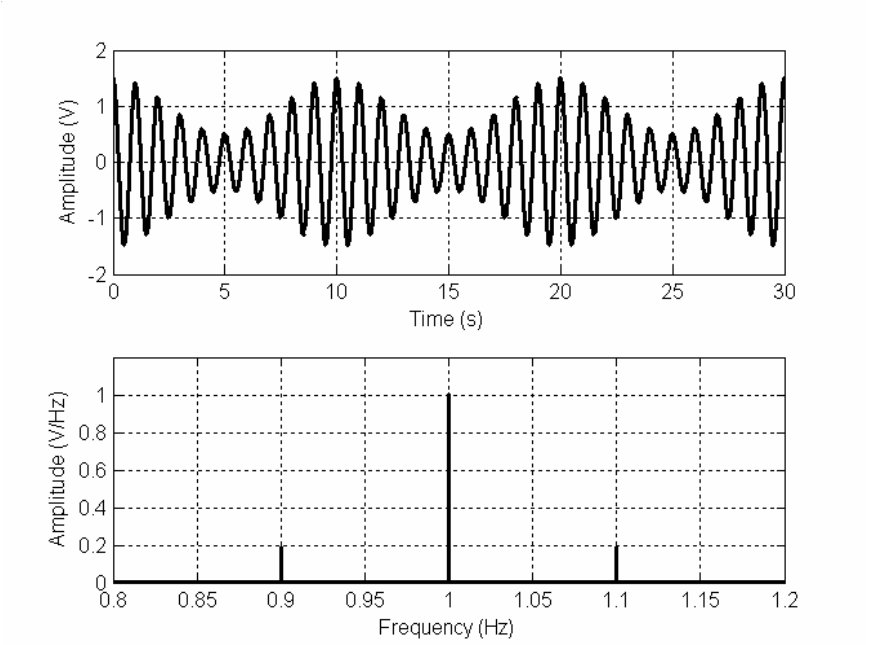

Figure 1: Example AM Signal in time and frequency domains

Figure 2: Acoustic duct environment

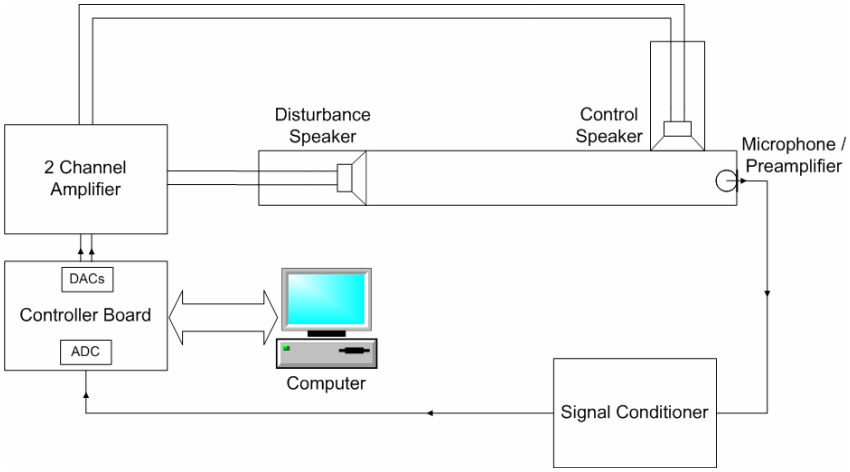

Figure 3: Experimental system block diagram

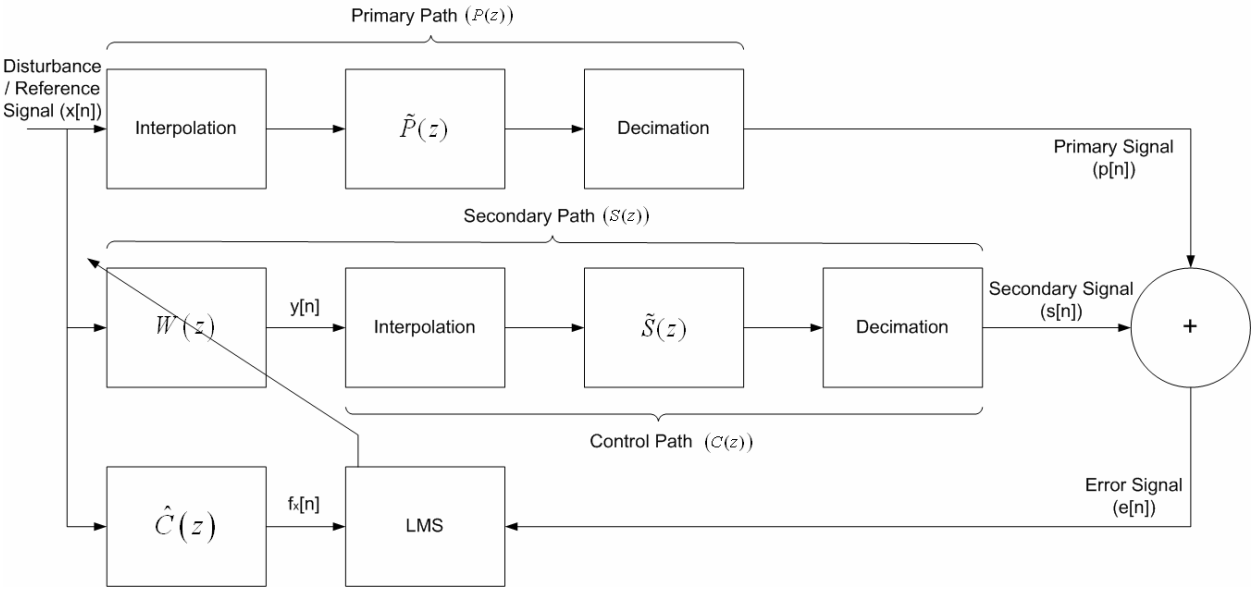

Figure 4: Block diagram of the FX-LMS algorithm implemented with oversampling

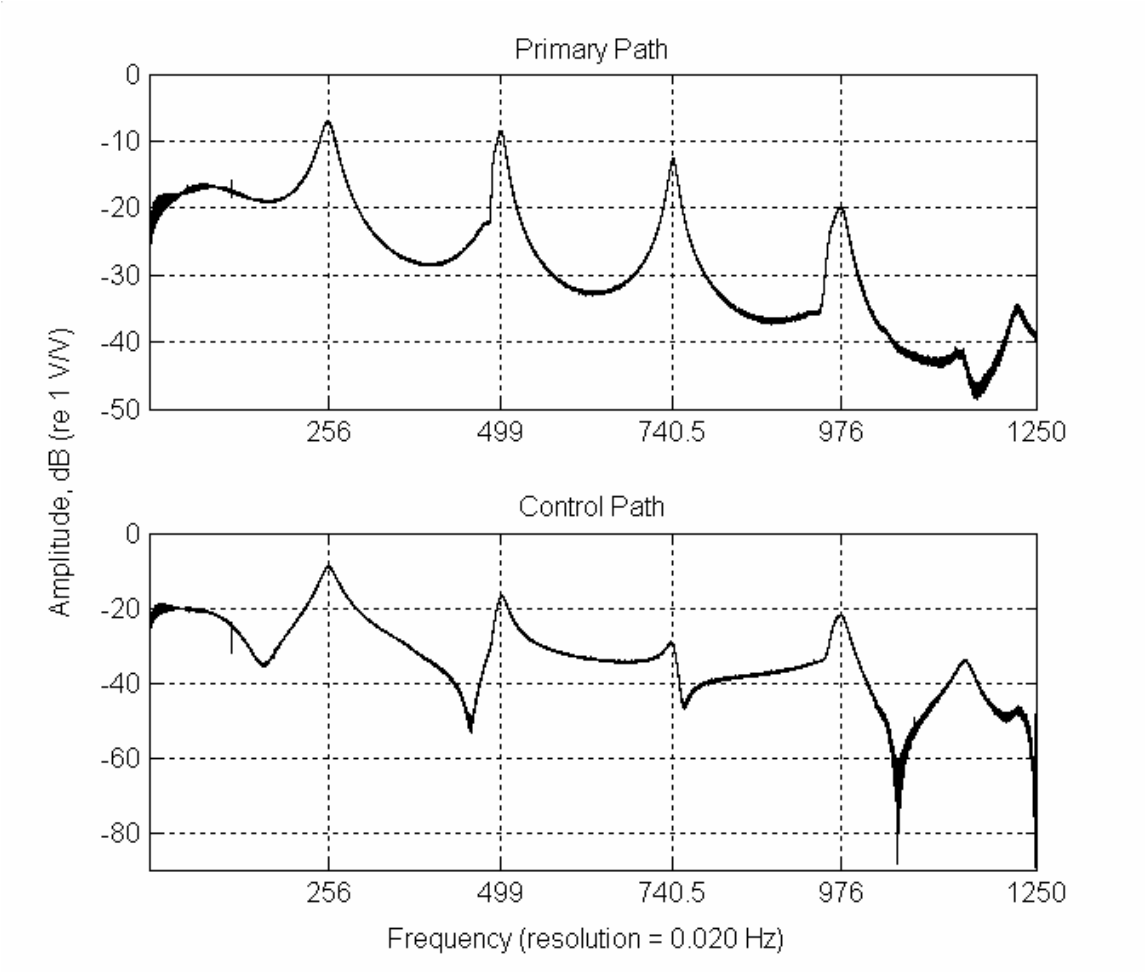

Figure 5: Magnitude frequency response functions of the primary and control paths

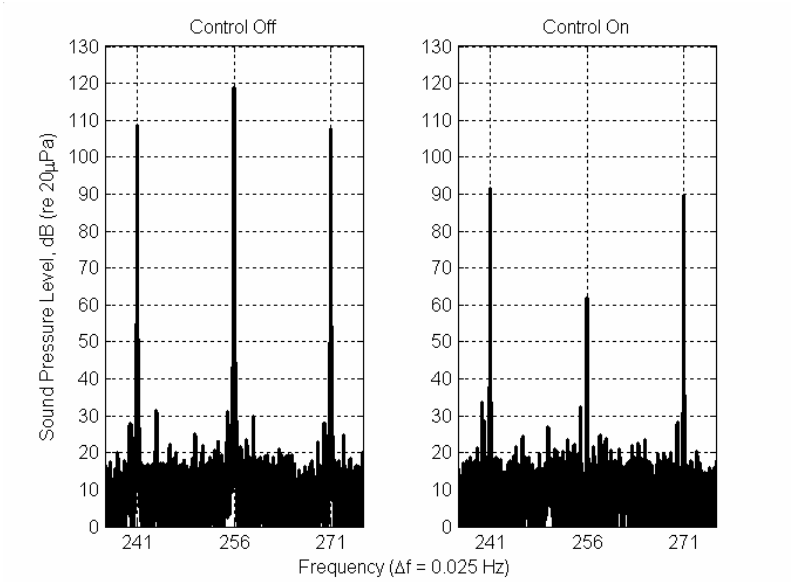

Figure 6: FX-LMS results, AM disturbance with on-resonance carrier

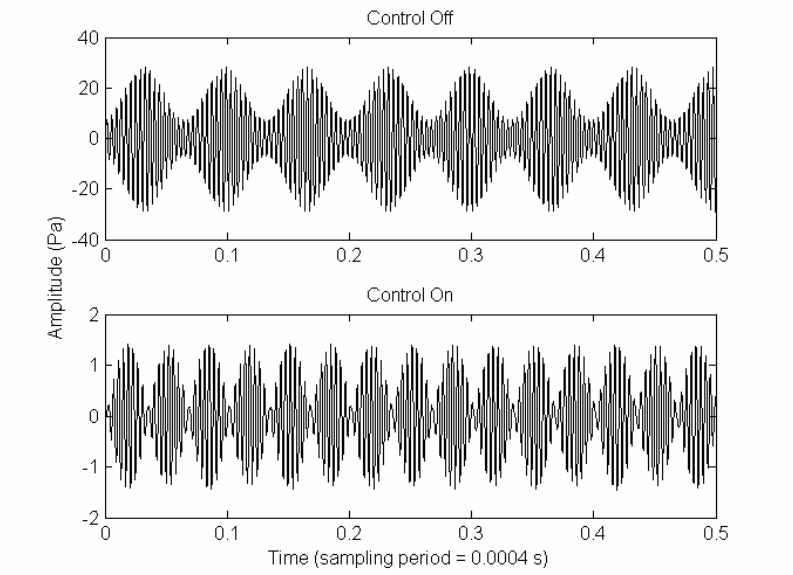

Figure 7: FX-LMS results, AM disturbance with on-resonance carrier

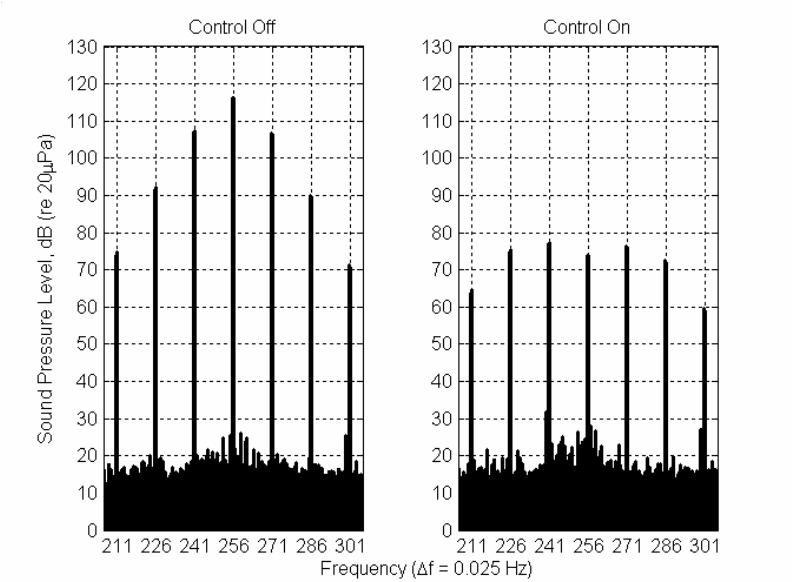

Figure 8: FX-LMS results, FM disturbance with on-resonance carrier

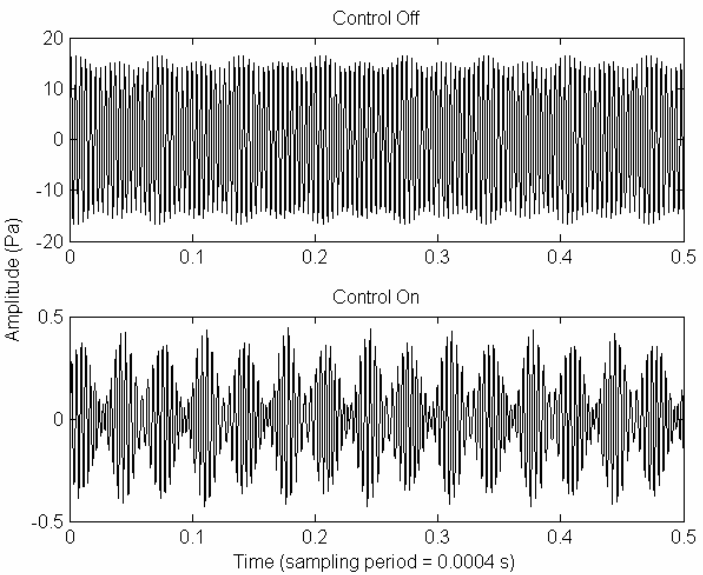

Figure 9: FX-LMS results, FM disturbance with on-resonance carrier

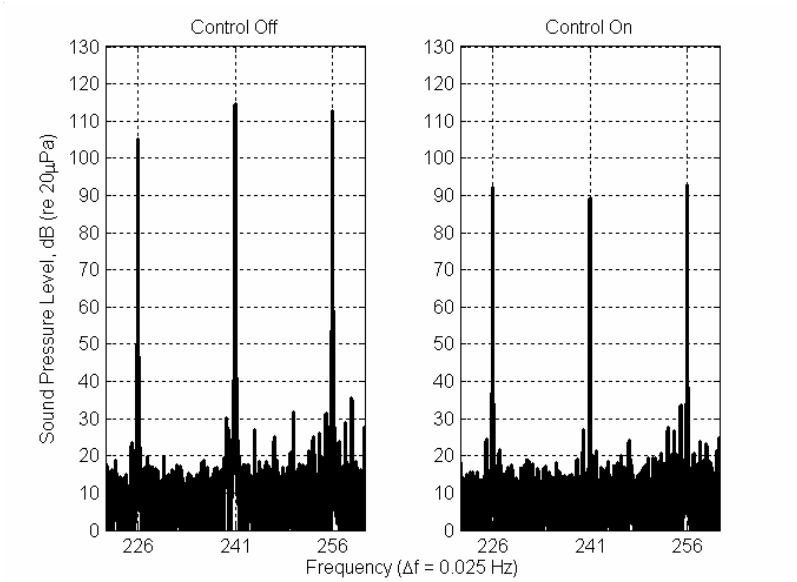

Figure 10: FX-LMS results, AM disturbance with on-resonance side-band

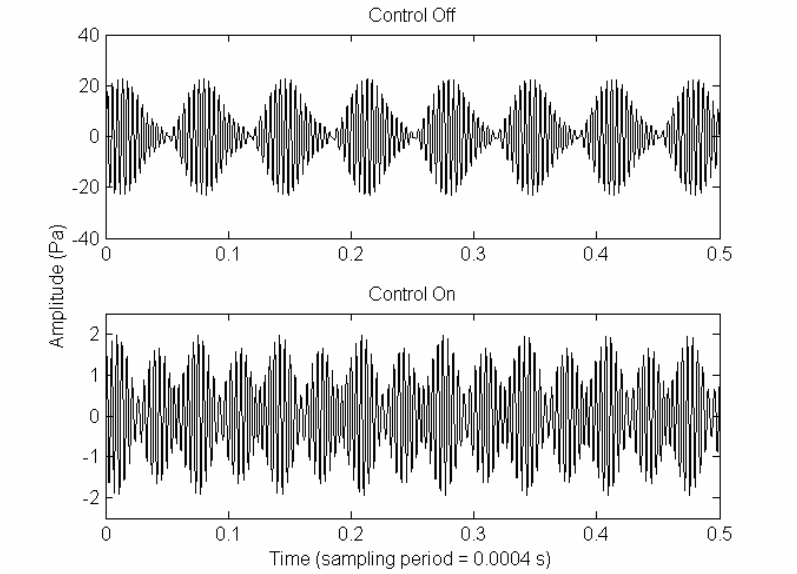

Figure 11: FX-LMS results, AM disturbance with on-resonance side-band

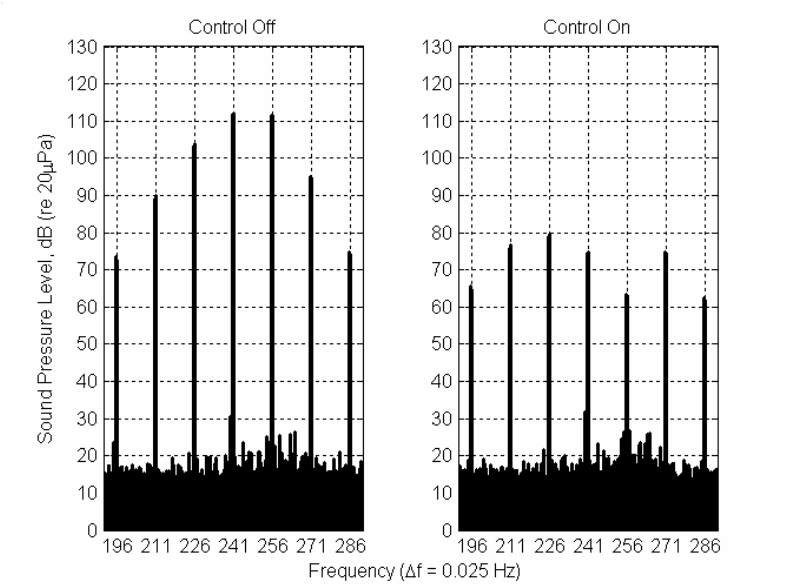

Figure 12: FX-LMS results, FM disturbance with on-resonance side-band

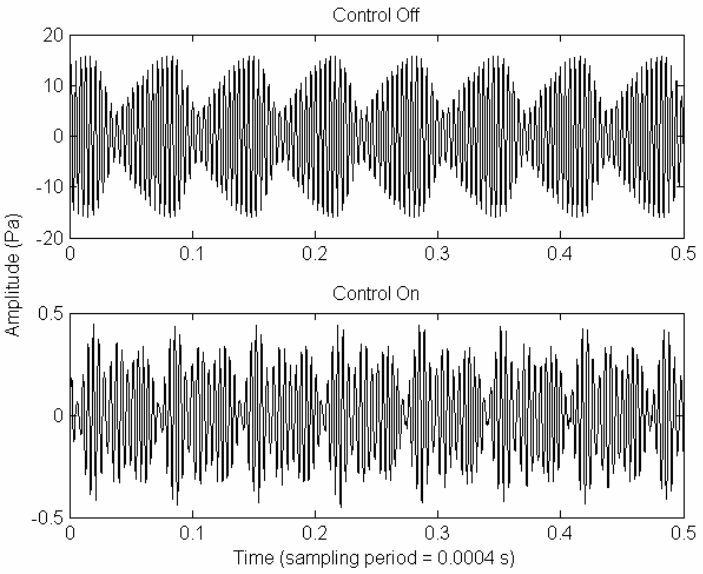

Figure 13: FX-LMS results, FM disturbance with on-resonance side-band

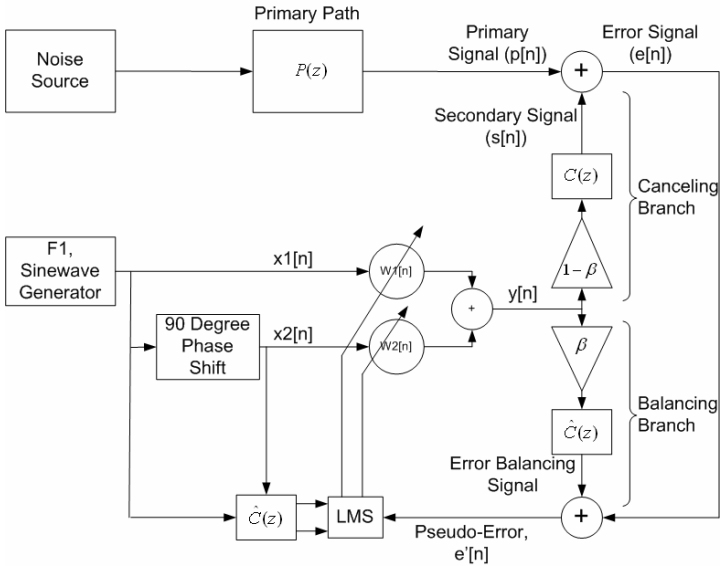

Figure 14: Block diagram of the Single Frequency NANE

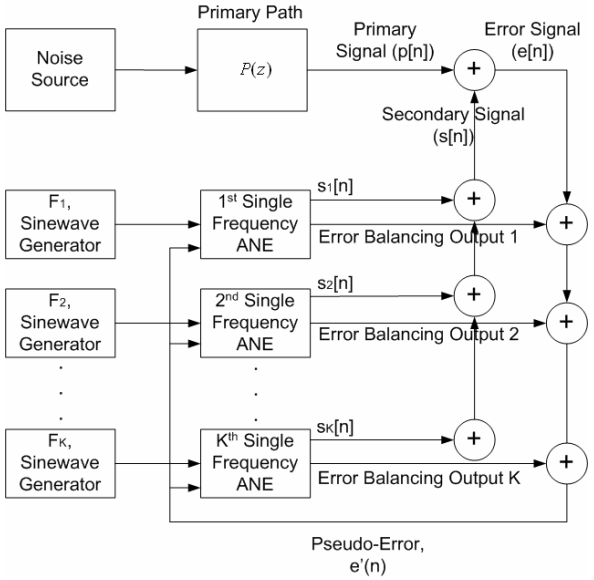

Figure 15: Block diagram of the Multiple Frequency NANE

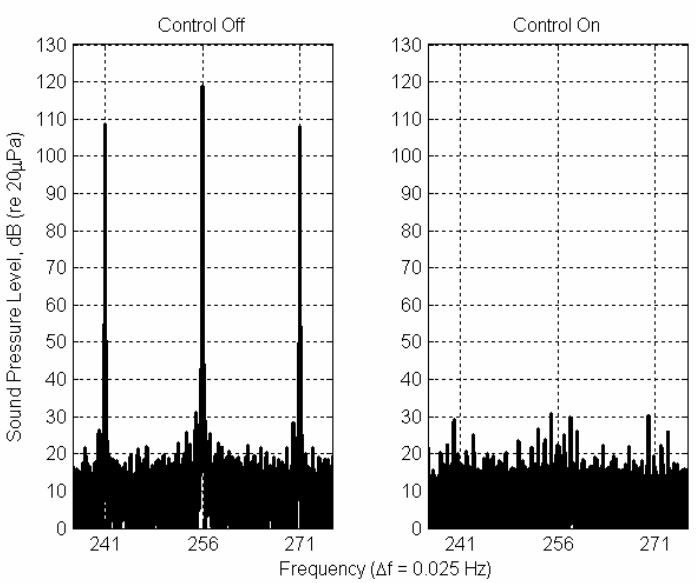

Figure 16: NANE results, AM disturbance with on-resonance carrier

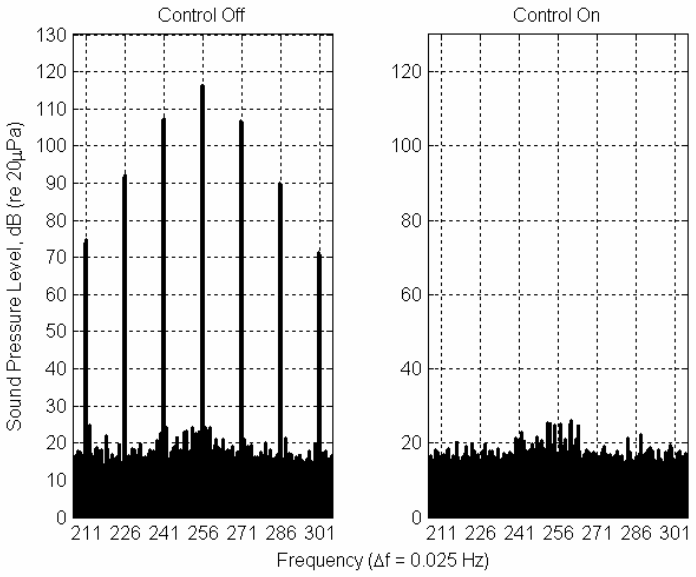

Figure 17: NANE results, FM disturbance with on-resonance carrier

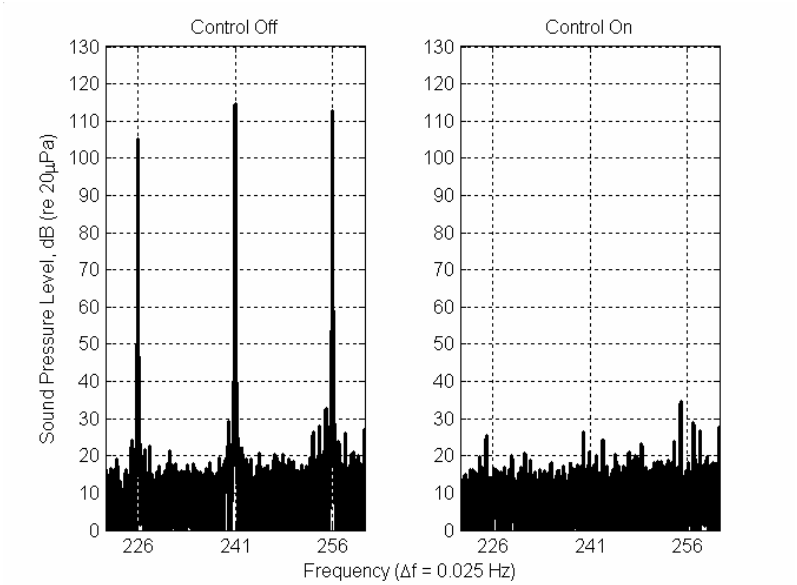

Figure 18: NANE results, AM disturbance with on-resonance side-band

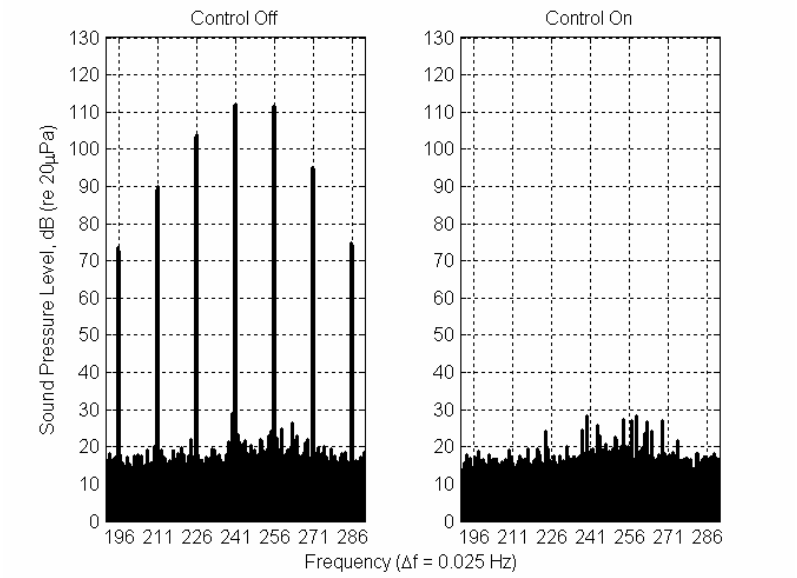

Figure 19: NANE results, FM disturbance with on-resonance side-band

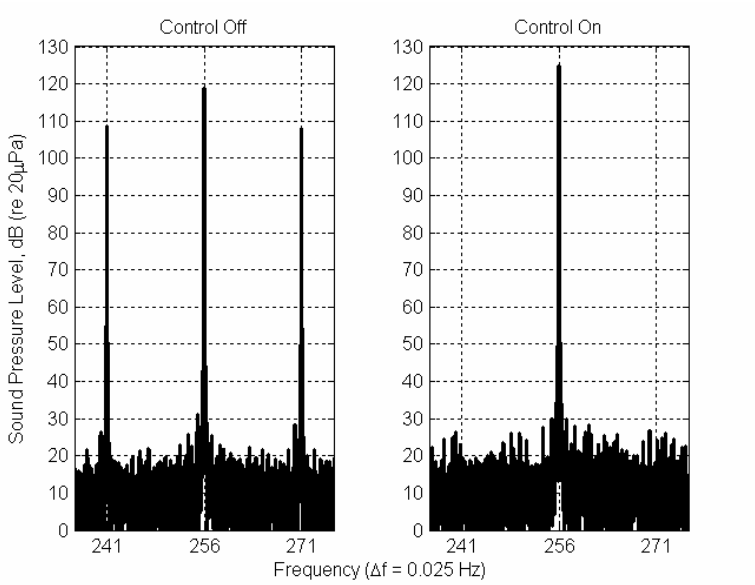

Figure 20: Spectral shaping using the NANE

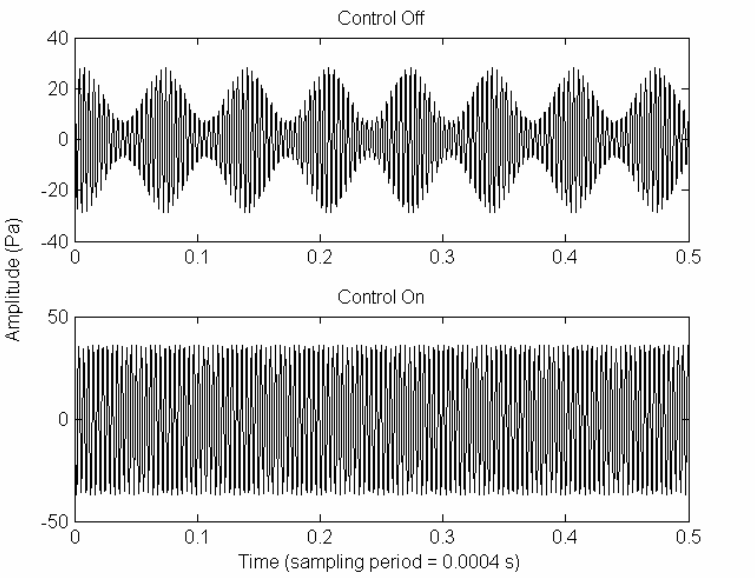

Figure 21: Resulting time history from spectral shaping